

Supplemental Materials

Molecular Biology of the Cell

Bhandari et al.

SUPPLEMENTARY FIGURES

Figure S1. The loss of Glc7p and Pph21p activity does not lead to an increase in the soluble pool of Sec23p and Sec24p.

(A) Left, Lysates (T) prepared from wild type (SFNY1309; lanes 1-3) and the *glc7-10* (SFNY1308; lanes 4-6) mutant were centrifuged at 150,000xg to generate supernatant (S) and pellet (P) fractions. Bos1p is shown as a fractionation control. Right, quantitation of the data in Figure S1A, left. Error bars represent the S.E.M, N=3. (B) Quantitation of Figure 1B (left). The ratio of supernatant:pellet for each coat subunit in wild type and the *sit4Δ* mutant is reported. Error bars represent the S.E.M, N=3. * $P < 0.05$; ** $P < 0.01$ Student's *t*-test. (C) Quantitation of Figure 1B (right). Error bars represent the S.E.M, N=3.

Figure S2. Lst1p and Sec31p are phosphorylated by Hrr25p.

(A) Sec31p is hyperphosphorylated in the *sit4Δ* mutant. Sec31p was immunoprecipitated from wild type (SFNY 1841) and the *sit4Δ* mutant (SFNY 2045) and incubated at 37°C for 15 min (lanes 1,4) with CIP (lanes 2, 5) or CIP with EDTA (lanes 3, 6) before the samples were analyzed on a 6% SDS polyacrylamide gel by Western blot analysis. (B) Hrr25p phosphorylates Lst1p and Sec31p in vitro. GST-Lst1p, GST (Left), GST-Sec31p (amino acids 1-500) and GST-Sec13p (Right), were incubated without (lane 1), or with His₆-Hrr25p (lane 2) or His₆-Hrr25p K38R (lane 3) in a kinase assay buffer containing γ P³²-ATP. The autoradiograms and coomassie-stained gels are shown. (C). Hrr25p phosphorylates Lst1p in vivo. Lysates from wild type (SFNY2051), the *hrr25-5*

(SFNY2049), and *sit4Δ* (SFNY2179) mutants and the *hrr25-5 sit4Δ* double mutant (SFNY2178) were analyzed on a 6% SDS polyacrylamide gel that was immunoblotted with anti-Lst1p antibody. A description of the isolation of the *hrr25-5* mutant is provided in the supplemental information. Lst1p was resolved as a doublet in wild type (lane 1) that migrated faster in the *hrr25-5* mutant (lane 2) and slower in the *sit4Δ* mutant (compare lanes 1-3). In the *sit4Δ* mutant the higher molecular weight band was more prominent. In the *hrr25-5 sit4Δ* double mutant, however, the relative intensities of the two bands were almost equal (compare lanes 3 and 4). Please note that the doublet of Lst1p seen in wild type is not always resolved on gels. Together these findings support the proposal that Hrr25p phosphorylates Lst1p in vivo. Bos1p is shown as a loading control. (D) Sit4p binds to Sec23p and Sec24p in vitro. Equimolar amounts (0.2μM) of GST-Sec23p, GST-Sec24p and GST-Sec13p were incubated with Sit4p (0.2μM), washed, and analyzed by Western blot analysis using anti-His antibody. GST and GST-Sec13 served as negative controls.

Figure S3. Sit4p binds directly to Hrr25p.

(A) The *sit4Δ* mutant displays a slow growth phenotype. WT and the *sit4Δ* mutant were grown on YPD plates at 25°C for 6 days. (B) The *sit4Δ* mutant fails to grow in the absence of *SSD1*. The *sit4Δ* mutant (1, *MATa GAL+ ura3-52 leu2-3,112 his3Δ200 sit4Δ::His3MX6*) containing pRS316-*SIT4* (CEN-*URA3*) and three different transformants of the *sit4Δssd1Δ* double mutant (2-4; *MATa GAL+ ura3-52 leu2-3,112 his3Δ200 sit4Δ::His3MX6 ssd1Δ::KanMX6* containing pRS316-*SIT4* (CEN-*URA3*) were purified on SC-Ura or 5-FOA plates. The SC-Ura plate was incubated at 25°C for 5 days, while the 5-FOA plate was incubated at 25°C for 14 days. (C) Increasing amounts of

His₆-Sit4p were incubated with 0.2 μM of either GST (lanes 1-3) or GST-Hrr25p (lanes 4-6). Bound His₆-Sit4 was analyzed by Western blot analysis.

Figure S4. PP6 is largely soluble in HeLa and COS-7 cells.

(A) Quantitation of the data in Figure 4B, left. Error bars represent the S.E.M, N=3.

(B) Quantitation of the PP6 depletion in Figure 5A, left. Error bars represent the S.E.M., N=3. *** $P < 0.001$ Student's *t*-test. (C) COPI fragments in PP6 depleted cells. COS-7 cells were transfected with Mock, PP6 siRNA-07 (siPP6-07) or PP6 siRNA together with pCMV-Myc-hPPP6C-m3-07 (see Materials and Methods). The cells were immunostained with anti-COPI antibody (left panel) and the number of fragmented structures was quantified (right panel). Error bars represent the SEM, N=3. Greater than 100 cells were examined in three independent experiments. *** $P < 0.001$ Student's *t*-test. Scale bar represents 20 μm. (D) Quantitation of the PP6 depletion in Figure 6. Error bars represent the S.E.M., N=3. *** $P < 0.001$ Student's *t*-test.

Figure S5. PP6 functions in Golgi reformation following the removal of BFA.

COS-7 cells were transfected with PP6 siRNA or mock transfected with lipofectamine reagent alone and grown for three days. Cells were then either fixed directly (“untreated”) or incubated for 1 hr with BFA, followed by fixation (“0 min washout”) or recovery in normal medium for 75 min prior to fixation (“75 min washout”).

Representative widefield fluorescence images are shown from each condition. Scale bar represents 25 μm.

REFERENCE

Muhlrad, D., Hunter, R., and Parker, R. (1992). A rapid method for localized mutagenesis of yeast genes. *Yeast*. 8, 79-82.

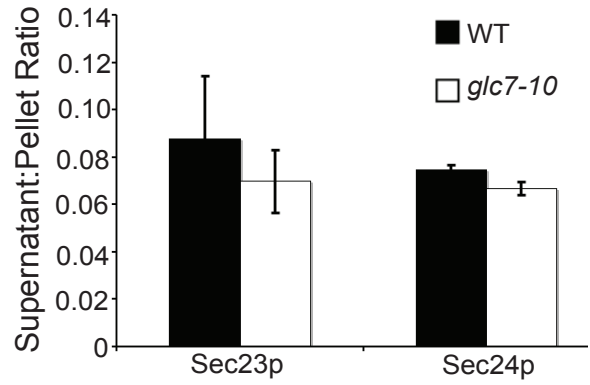
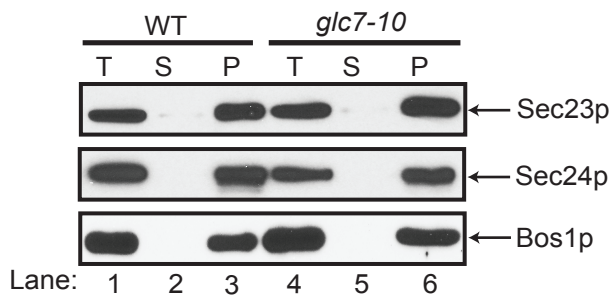
Table S1: Bacterial strains used in this study

Strain Number	Plasmid	Source
SFNB1337	pGEX-4T2- <i>SEC13</i> , Amp ^R	This study
SFNB1346	pGEX-2T- <i>SEC23</i> , Amp ^R	Randy Schekman
SFNB1462	pGEX-2T- <i>SEC24</i> , Amp ^R	Chris Kaiser
SFNB1486	pGEX-4T3- <i>SEC31</i> (aa1-500), Amp ^R	This study
SFNB1714	pCMV-Myc-DDK-CSNK1D, Amp ^R	Origene
SFNB1715	pRS315- <i>HRR25</i> (CEN <i>LEU2</i>), Amp ^R	This Study
SFNB1724	pGEX-4T2- <i>HRR25</i> , Amp ^R	This Study
SFNB1781	pGEX-4T2- <i>SEC31</i> (aa879-1114), Amp ^R	This Study
SFNB1805	pET28a- <i>SIT4</i> , Kan ^R	This Study
SFNB1860	pGEX-4T2- <i>SEC31</i> (aa501-878), Amp ^R	This Study
SFNB1861	pGEX-4T2- <i>SEC31</i> (aa1115-1273), Amp ^R	This Study
SFNB1888	pGEX-6P1- <i>LST1</i> , Amp ^R	This Study
SFNB1905	pRS316- <i>SIT4</i> (CEN <i>URA</i>), Amp ^R	This Study
SFNB1912	pNB530- <i>GAL1pr-SIT4</i> (<i>URA</i>), Amp ^R	This Study
SFNB1947	pET3a- <i>HRR25</i> (aa2-394), Amp ^R	Kevin Corbett
SFNB1948	pET3a- <i>HRR25_K38R</i> (aa2-394), Amp ^R	Kevin Corbett

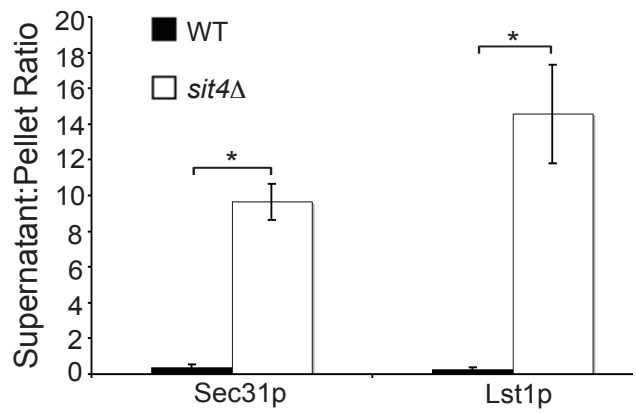
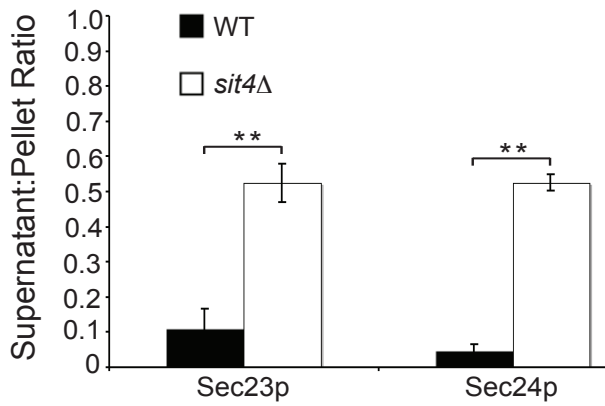
Table S2: Yeast strains used in this study

Strain Number	Genotype	Source
SFNY1942	<i>Mat a/α his3Δ1/ his3Δ1 MET15/met15Δ0 LYS2/lys2Δ0 ura3Δ0/ura3Δ0 leu2Δ0/leu2Δ0 HRR25/hrr25Δ::KanMX6</i>	Open Biosystems
SFNY1968	<i>Mat α his3Δ1 met15Δ0 ura3Δ0 leu2Δ0 hrr25Δ::KanMX6 pRS316-HRR25(URA3+)</i>	This study
SFNY2049	<i>MATα ura3Δ0 leu2Δ0 met15Δ0 his3Δ1 hrr25Δ::KanMX6 pRS315-hrr25-5(LEU2+)</i>	This study
SFNY2178	<i>MATα ura3Δ0 leu2Δ0 met15Δ0 his3Δ1 hrr25Δ::KanMX6 pRS315-hrr25-5(LEU2+) sit4Δ::His3MX6</i>	This study

A



B



C

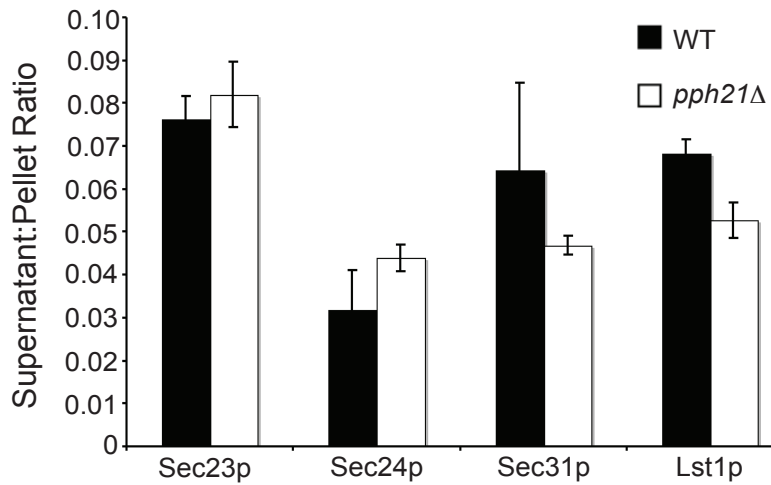
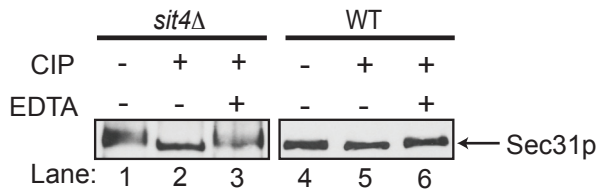
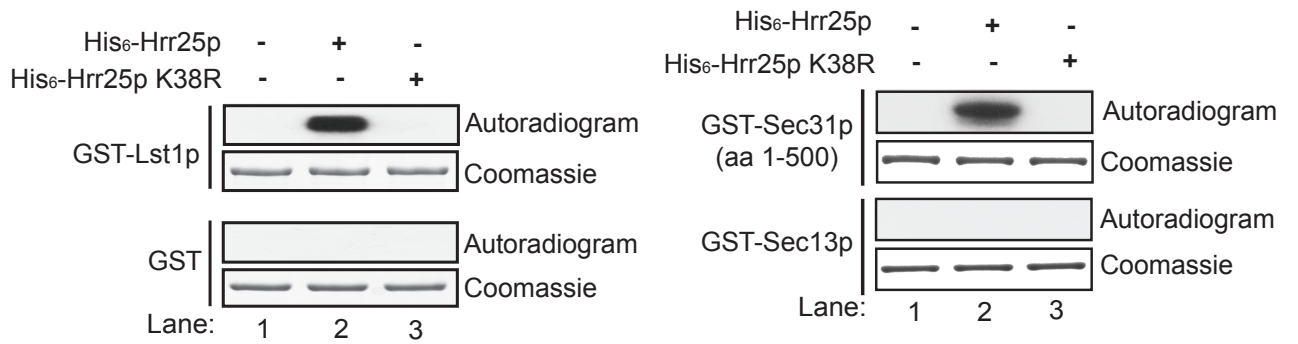


Figure S1

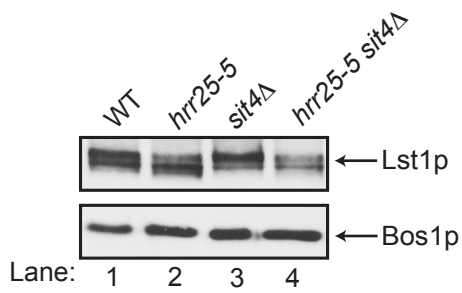
A



B



C



D

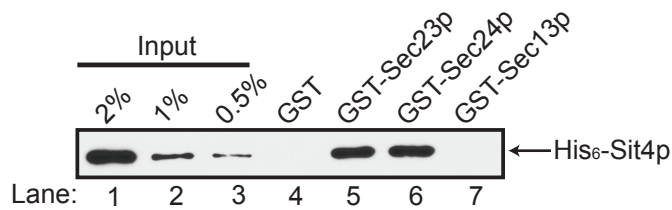
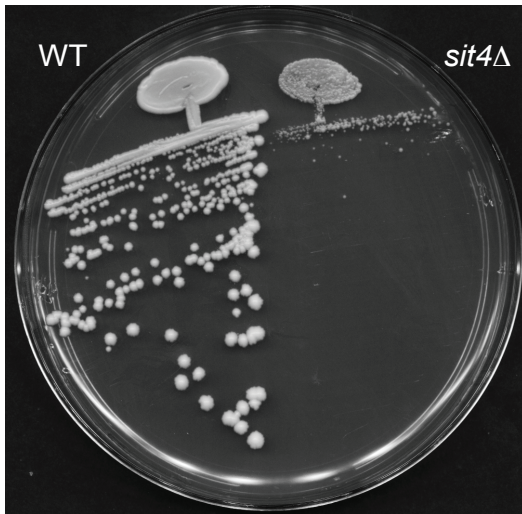
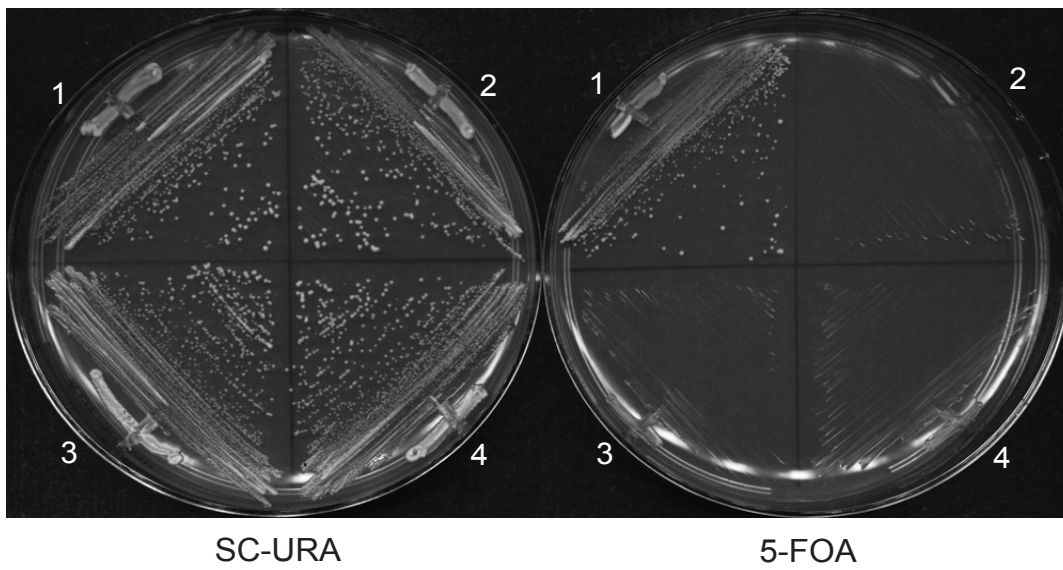


Figure S2

A



B



C

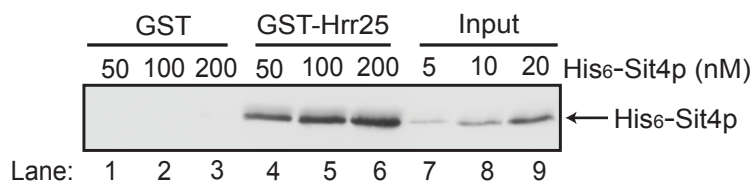
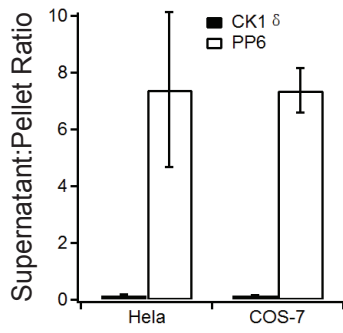
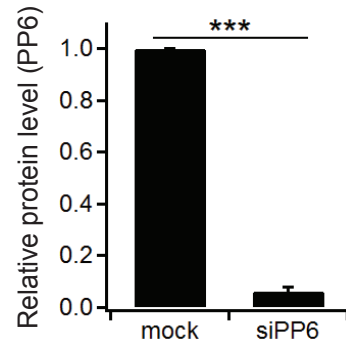


Figure S3

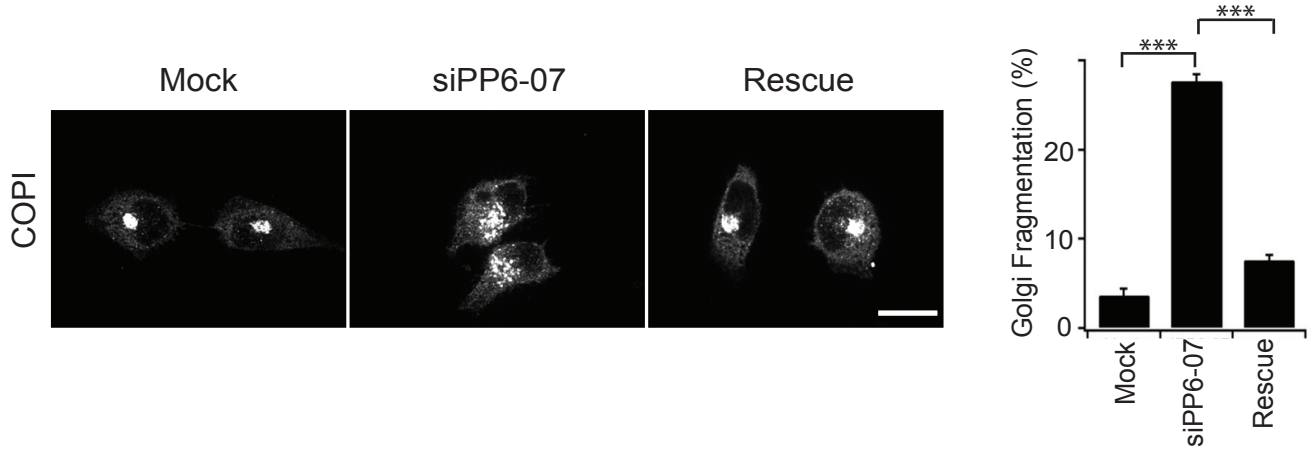
A



B



C



D

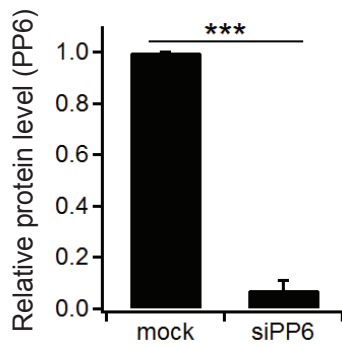


Figure S4

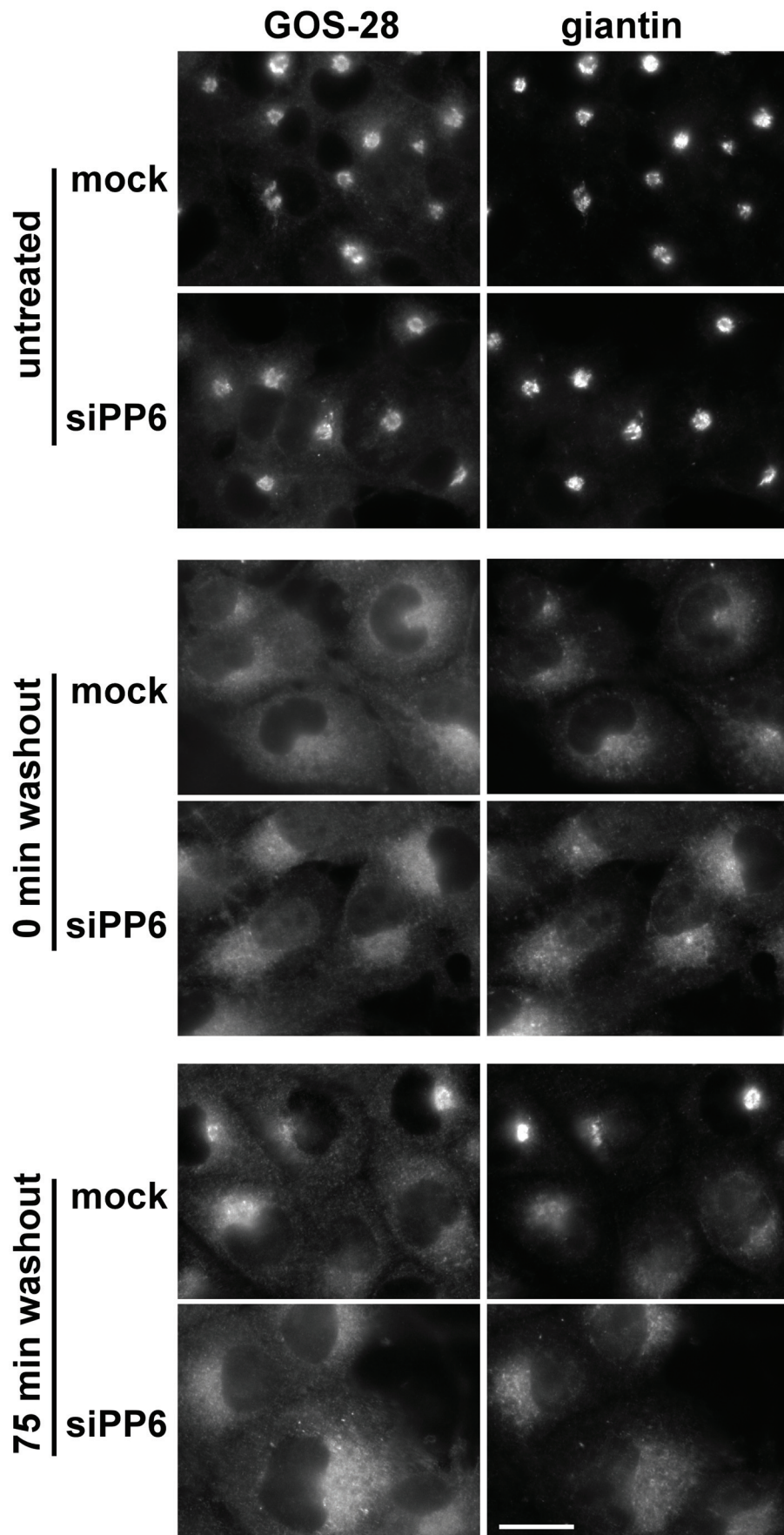


Figure S5